# Modulated structures of the smectic-$C^*$ phase in free-standing films with high spontaneous polarization

E.I. Demikhov, E. Hoffmann, and H. Stegemeyer
*Institute of Physical Chemistry, University of Paderborn, 33095 Paderborn, Germany*

S.A. Pikin
*Institute of Crystallography, Russian Academy of Sciences, Moscow, Leninsky Prospect 59, 117333 Russia*

A. Strigazzi
*Dipartimento di Fisica, Politechnico di Torino, Corso Duca degli Abruzzi 24, I-10129 Torino, Italy*
(Received 30 November 1994)

The stripe instability of smectic-$C^*$ free-standing films with high spontaneous polarization is studied experimentally and theoretically. By variation of the temperature, the number of smectic layers, and the spontaneous polarization in chiral-racemic mixtures, different structural states develop in the film. Temperature–number-of-layers phase diagrams of the smectic-$C^*$ structural states with spontaneous polarization as a parameter have been measured. The critical number of layers and spontaneous polarization for the textural transformations have been determined. A stripe state has also been observed in an antiferroelectric phase. A mechanism for stripe formation is proposed that considers the stripes occurring as flexoelectric instabilities in an electric field inherently produced by the film. The proposed theoretical model gives a qualitatively good explanation of the experimental data.

PACS number(s): 64.70.Md, 68.15.+e, 77.80.−e

## I. INTRODUCTION

Free-standing films of smectic liquid crystals [1–5] are unique experimental objects for the investigation of properties depending on the number of layers. Recent progress in this area has been combined with the investigation of surface ordering phenomena [6] and dimensional crossover effects [7–9]. In spite of these developments, ferroelectric smectic liquid crystals in two dimensions have only rarely been studied. In early experimental works [1, 2], the spontaneous polarization in free-standing films of the classic ferroelectric liquid-crystalline substance *p*-decyloxybenzylidene-*p'*-amino-2-methylbutylcinnamate (DOBAMC) has been measured and was found to be consistent with bulky studies. Spontaneous formation of a weakly anisotropic state in two-dimensional ferroelectric films has been predicted in [10–12] to be caused by suppression of thermal fluctuations by dipolar interaction. Different types of molecular packings in ferroelectric and antiferroelectric phases have been studied in ultrathin films [13]. Periodic textures in free-standing smectic-$C^*$ films with high spontaneous polarization have been reported in [14].

The geometry of free-standing smectic films provides experimental possibilities for observations of thermodynamically stable structures that do not exist under fixed boundary conditions for the azimuth angle on solid substrates. Two different kinds of periodically modulated structures have been recently observed in free-standing films. One- and two-dimensionally modulated patterns have been found in thin free-standing films with the number of layers $N \leq 60$ of achiral smectic-$C$ phase [15, 16]. These textures have been explained as a consequence of chiral symmetry breaking inside the boundary layers [16, 17]. This symmetry breaking takes place because of the coupling of the chirality order parameter with the director field bend deformation. In [18] it has been shown that the basic structure state of the free boundary of the achiral smectic-$C$ films is analogous to that of surfactant monolayers [19–21].

The stripe state in free-standing films of the ferroelectric smectic-$C^*$ phase [14] has been observed in thick films ($N \geq 85$) of materials with high spontaneous polarization [22]. In this paper the formation of different structural states in free-standing smectic-$C^*$ films as a function of temperature, number of layers, and spontaneous polarization in chiral-racemic mixtures has been investigated. In previous theories of modulated structures in free-standing films [16, 23, 24] important features have not been discussed. First of all, an electric field perpendicular to the smectic layers, which is always present in experiments, has to be taken into account. This field can originate from (i) surface effects and (ii) mechanical film deformation. Coupling between the electric field and the director can result in periodic distributions of polarization vectors [25] similar to well known flexoelectric instabilities [12]. This effect should depend on the value of the flexoelectric constant, which even in achiral smectic phases can be very large [25]. In this paper a model is proposed that describes the experimental properties of the stripe state in free-standing films of chiral smectic-$C^*$ phase.

 

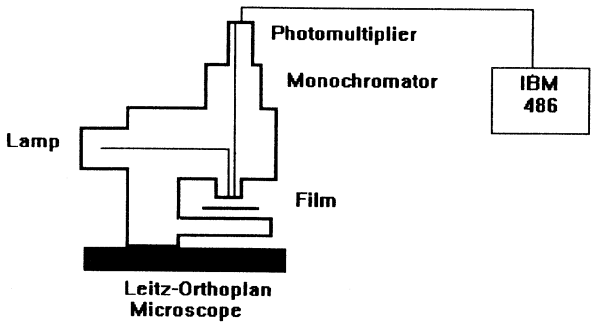


FIG. 1. Scheme of the experimental setup.

## II. EXPERIMENTAL SETUP

Chiral 4-(2S,3S)-2-[chloro-3-methylpentanoyloxy]-4′-heptyloxybiphenyl ($C7$) and its chiral-racemic mixtures have been studied. This substance possesses the following liquid-crystalline phases: isotropic (62 °C) smectic-$A$ (54.6 °C) smectic-$C^*$ (43 °C) smectic $G$ [26]. The spontaneous polarization in the smectic-$C^*$ phase of pure chiral $C7$ varies between 130 and 290 nC/cm$^2$ with decreasing temperature. The first-order smectic-$A$–smectic-$C^*$ phase transition disappears in free-standing films thinner than $N_c \approx 15$ [8].

The scheme of the experimental setup is shown in Fig. 1. Films of $C7$ were drawn in a frame consisting of two brass rails and two movable brass blades. Films with homogeneous thickness were produced in the smectic-$A$ phase and cooled down to the smectic-$C^*$ phase. The $C7$ free-standing film properties were studied in a broad interval of a number of layers (from 5 to 1000). Textures in free-standing films were investigated in a polarized Leitz-Orthoplan microscope between slightly decrossed polarizers and registered photographically. Our experimental setup enabled simultaneous optical observations and reflectivity measurements in the visible region of wavelengths. The number of smectic layers was determined by reflectivity measurements in the smectic-$A$ phase as described in [9]. An automatized monochromator was connected to the microscope and the recorded spectra were stored in a personal computer. The reflectivity spectra were fitted by an expression describing the multiple beam interference in a plane parallel plate [27]. Interlayer spacing in the smectic-$A$ phase was taken from the x-ray measurements in the smectic-$A$ phase of $C7$ [26]. The applied method allows the exact determination of the number of layers in a broad interval of film thicknesses and the refractive index [9]. Spontaneous polarization was measured with a common triangle wave method in bulky samples.

## III. EXPERIMENTAL RESULTS

Figures 2(a) and 2(b) show the $N/T$ phase diagram of smectic-$C^*$ structural modifications in pure chiral $C7$ [Fig. 2(a)] and in a chiral-racemic mixture with an 85% chiral component [Fig. 2(b)]. In thick films ($N \geq 85$) of chiral $C7$ two textures have been observed. An anisotropic state occurs close below the phase transition Sm-$A$–Sm-$C^*$ after annihilation of defects over approximately 0.5–1 h. On subsequent cooling, a stripe state occurred. The anisotropic state is characterized by a homogeneous contrast between crossed polarizers, which is changed by a rotation of the microscope table. The anisotropic state temperature interval increases with a decreasing number of layers. In films thinner than 85 layers the stripe state disappears. Defect-free ultrathin films were produced from very thick films by successively removing smectic layers over 2–3 h. During this process each film was cooled to the smectic-$C^*$ phase and annealed over 10–15 min. Anisotropic, relaxed structures in thick and thin films of $C7$ cannot be distinguished in the optical microscope. The difference between the annealed textures of the anisotropic state in thick and ultrathin films is related to the structure occurring around defects. The variation of the contrast around defects in the anisotropic state in thick films is always smooth [14]. Discontinuous defect walls of different configurations are typical for ultrathin films ($N \leq 30$) just after the cooling from the smectic-$A$ phase. One of the possible configurations of the anisotropic state in films with fewer than 30 layers is the "chessboard" texture observed in [14]. However, we have not succeeded in producing this tex-

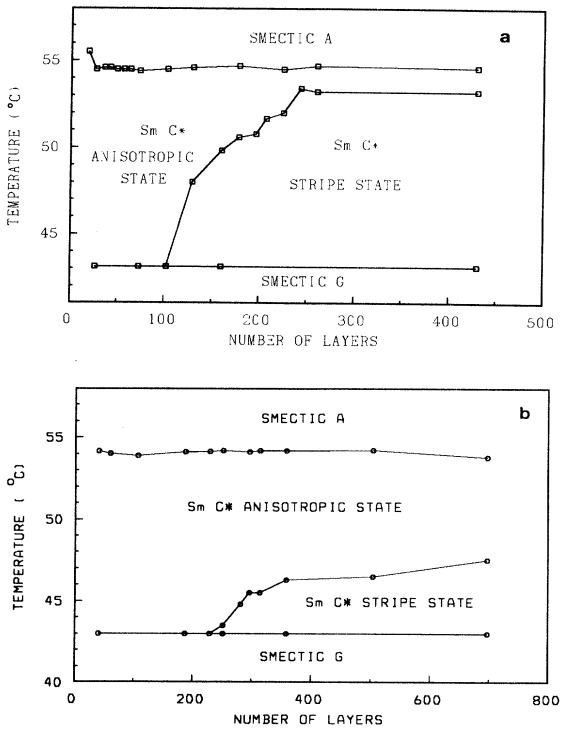


FIG. 2. (a) $N/T$ phase diagram of chiral $C7$ and (b) chiral-racemic mixture with 85% chiral component. The solid line shows fitting of the dependence of $T_s$ on a number of layers with Eq. (12). The dotted line is the boundary between anisotropic textures in thick and ultrathin films.

ture over the whole film area. Figure 3 shows another metastable structure with aperiodic stripes. This state is characterized by a constant contrast inside the stripes. The anisotropic state with discontinuous walls has been found only in mixtures with more than 95% chiral $C7$. Relaxation of defect walls is a very slow process and the texture of Fig. 3 is quasistable. A decrease of the chiral component concentration increases the temperature interval of the anisotropic state in thick films, as shown in Fig. 2(b). Textures in thin and thick films of the smectic-$C^*$ phase are modifications of the schlieren for the chiral component concentration less than 75%. There is no difference in the director field configuration around defects between thick and thin films in this case. In a mixture with 75% chiral component the stripe state has not been observed. A further decrease of the chiral $C7$ concentration does not change the structure of the smectic-$C^*$ phase.

Figure 4 shows the variation of the relaxed textures of the anisotropic state on decreasing chiral $C7$ concentration. Figure 4(a) presents an image of spontaneously oriented anisotropic state in ultrathin films ($N \approx 30$) of pure chiral $C7$ in which a small defect region is seen and disappears with time. As already mentioned, there is no difference between structures of the anisotropic state in thick and thin films in pure chiral $C7$. Figure 4(b) shows an anisotropic texture in a 150-layer film of a mixture with 87.5% chiral component. Figure 4(c) presents a typical schlieren texture of the smectic-$C^*$ phase of a mixture with 50% chiral $C7$.

A stable stripe state occurs spontaneously in thick films ($N \geq 85$) of mixtures with chiral $C7$ concentration 75–100% on cooling at a temperature $T_s$ below the Sm-$A$–Sm-$C^*$ phase transition (Fig. 5). The dependence of $T_s$ on the number of layers for two mixtures is shown in Fig. 2. The region of the stripe state in the phase diagram decreases with decreasing chiral $C7$ concentration. The anisotropic state–stripe state structural transformation is reversible: the stripe texture disappears on heating 1–3 °C above $T_s$. Usually the stripe texture is deformed and it is difficult to ascribe some characteristic periodicity to this state. The stripe texture can be aligned by the motion of the movable side of the film frame parallel to it.

Figure 6 shows the temperature dependence of the interstripe spacing for some pattern with perfect stripe orientation on cooling and heating. The stripe periodicity decreases with decreasing temperature. The tempera-

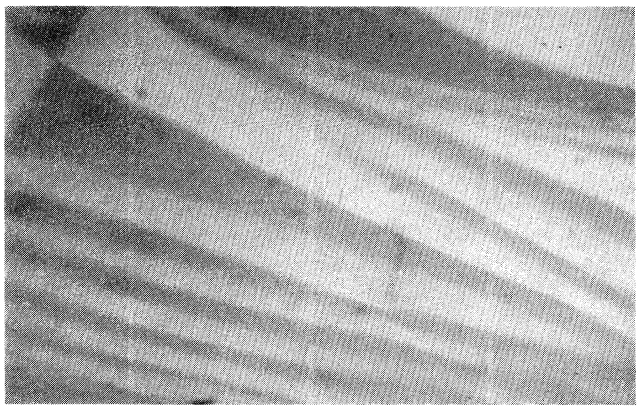

FIG. 3. Metastable anisotropic texture in a 25-layer film at $T = 48.06$ °C.

(a)

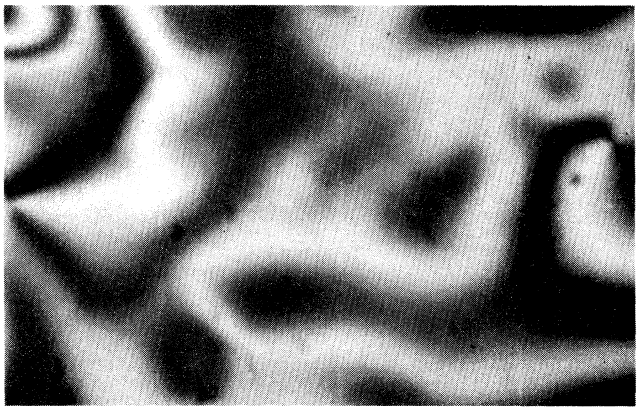

(b)

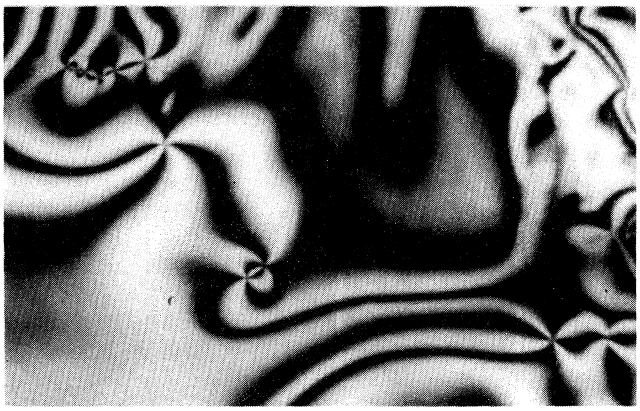

(c)

FIG. 4. (a) Anisotropic texture of a $N$=30 smectic-$C^*$ film of 100% chiral $C7$ at $T = 48.06$ °C. (b) Anisotropic smectic-$C^*$ texture of an $N$=150 film of 87.5% chiral $C7$ mixture at $T = 53.85$ °C; (c) Schlieren texture of thick films ($\sim$ 500 layers) in a mixture with 50% chiral $C7$ at $T = 50.05$°C.

ture hysteresis of the stripe periodicity is reminiscent of structural transformations during first-order phase transitions. Typical values of interstripe distance are relatively large ($\sim$ 80–150 $\mu$m). The stripe distance increases by lowering the chiral $C7$ concentration. The critical number of layers below which the stripe state is no longer stable ($N_{cr}$) increases with a decrease of chiral component concentration.

Figure 7 presents temperature dependences of spontaneous polarization for several mixtures. The behavior of spontaneous polarization is typical for the smectic-$C^*$ phase. At the smectic-$C^*$—smectic-$A$ transition point a small jump has been registered in mixtures with high spontaneous polarization. The Sm-$A$–Sm-C* transition in chiral $C7$ determined in these measurements is shifted to higher temperatures with respect to low chirality mixtures due to the coupling of $T_{AC}$ with the electric field.

Figure 8 shows the dependence of the critical number of layers ($N_{cr}$), where the stripe state disappears, on spontaneous polarization taken 5° below the Sm-$A$–Sm-$C^*$ transition temperature. The critical number of layers increases with a decrease of spontaneous polarization and diverges at approximately $P_s$=70 nC/cm$^2$.

Figure 9 shows the dependence of the spontaneous polarization at $T = T_s$ by $N \approx 500$ layers taken from Fig. 7 ($P_{cr}$) as a function of the chiral component concentration. It must be emphasized that there is no concentration dependence of this $P_S$ value with the accuracy of

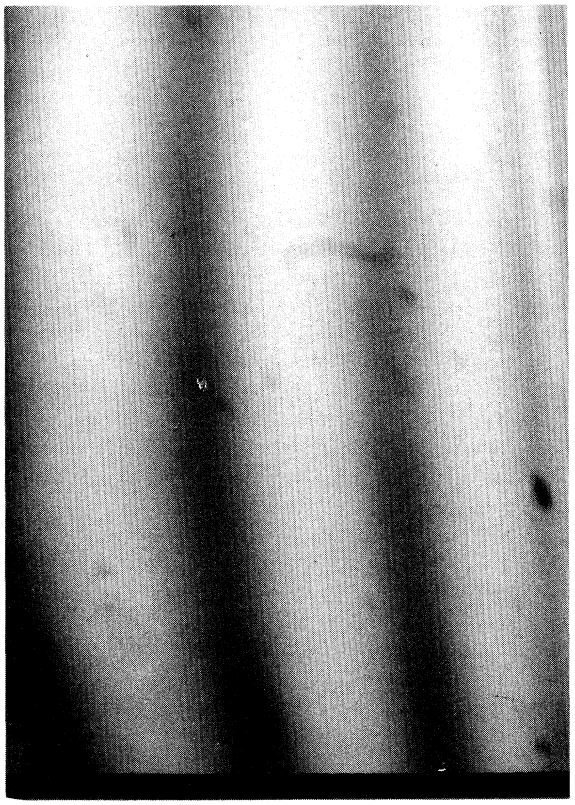

FIG. 5. Striped state of the plane director field of the smectic-$C^*$ phase in an $N$=400 film of chiral $C7$.

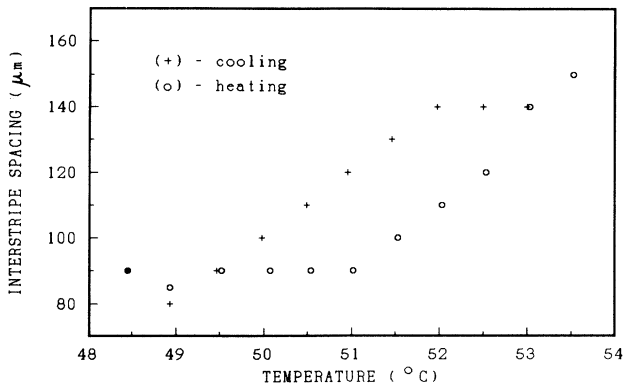


FIG. 6. Temperature dependence of the stripe periodicity for an $N$=243 film of $C7$.

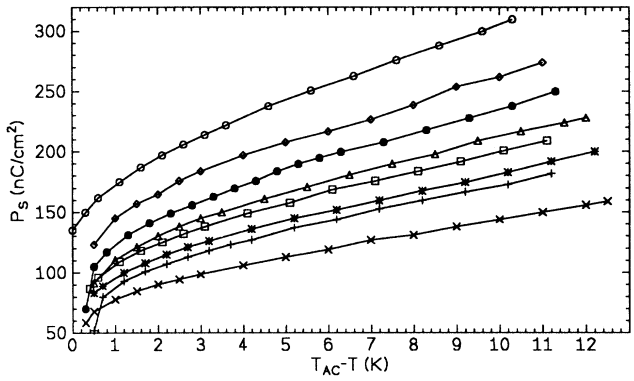


FIG. 7. Temperature dependence of spontaneous polarization for chiral-racemic mixtures of $C7$ with the following concentrations of the chiral component: 100% (○), 95% (◇), 92.5% (●), 87.5% (△), 85% (□), 82.5% (∗), 80% (+), and 75% (×).

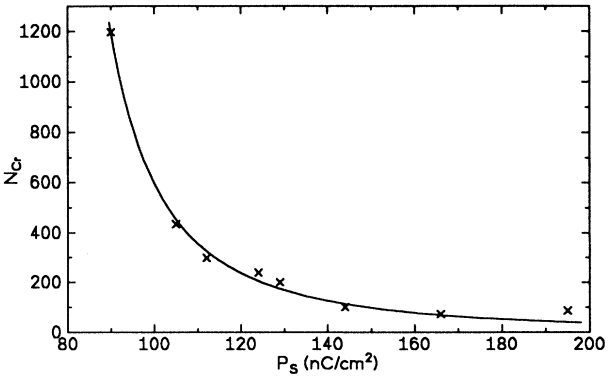


FIG. 8. Dependence of a critical number of layers for which the stripe state is not stable on spontaneous polarization.

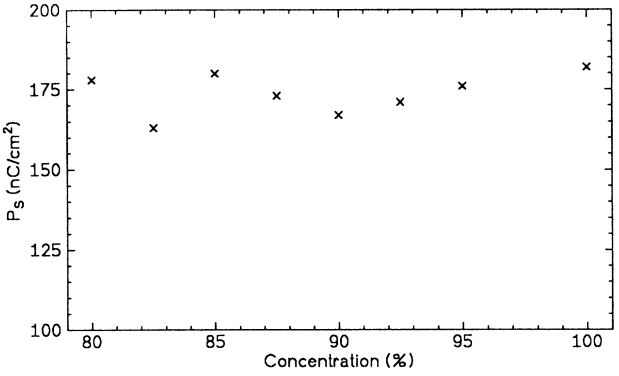


FIG. 9. Concentration dependence of spontaneous polarization at $T = T_s$ and $N \approx 500$ ($P_{cr}$).

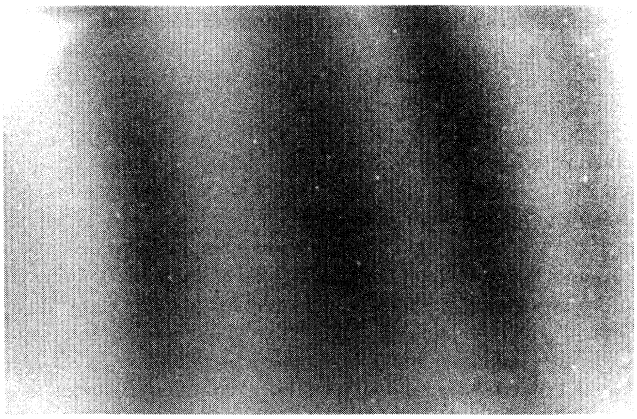

FIG. 10. Stripe state in an antiferroelectric phase of $Y1$.

our measurements. This plot gives the threshold spontaneous polarization that is necessary for the stripe state formation to $P_{cr} \approx 170 \pm 5$ nC/cm$^2$.

Textures in free-standing films of the 4-(2-methyloctanoyl)phenyl-4′-octyloxybiphenyl-4-carboxylate ($Y1$) have also been studied in the present work, which was synthesized by Yoshizawa and co-workers [28] and exhibits the following sequence of liquid-crystalline phases: isotropic (153.8 °C) smectic-$A$ (135.3 °C) smectic-$C^*$ (ferroelectric) (79 °C) smectic-$C_A$ (antiferroelectric) (50.3 °C) smectic $X$ (31.2 °C) cryst. The value of spontaneous polarization of this material is slightly larger than that of $C7$. Textures of smectic-$C^*$ free-standing films of $Y1$ observed by variation of the number of layers and temperature are similar to that of pure chiral $C7$. After the Sm-$A$–Sm-$C^*$ phase transition an anisotropic state was observed that was transformed into the stripe state at lower temperatures. The stripe state disappears in films thinner than 70 layers. The smectic-$C^*$ phase anisotropic textures in ultrathin films of $Y1$ differ by defect structures from thick films analogous to high spontaneous polarization mixtures of $C7$. After the Sm-$C^*$–Sm-$C_A$ phase transition in thick films the antiferroelectric phase possesses a domains structure with stripes inside. The periodicity of this stripe state is larger with respect to the smectic-$C^*$ phase. Figure 10 shows the stripe state in the antiferroelectric Sm-$C_A$ phase of $Y1$ after the recombination of domain walls. To observe this structure we cooled the films very slowly and after the Sm-$C^*$–Sm-$C_A$ phase transition sealed the films 1 h. Figure 10 shows the stripe texture inside one large domain approximately 300 $\mu m$ in diameter. In contrast to the Sm-$C^*$ phase, no domain walls were seen in the antiferroelectric phase in ultrathin films with $N \leq 30$. The texture of the antiferroelectric phase in this case is similar to the schlieren texture of smectic-$C^*$ of $C7$ mixtures with low spontaneous polarization. The Sm-$C^*$–Sm-$C_A$ phase transition does not disappear on decreasing the number of layers.

## IV. THEORETICAL MODEL

In this section, we shall consider the effects of external fields on the in-plane modulations for smectic-$C$ films. Generally, if an external field $E$ is applied normally to the film surface, the component $E_z$ should be included in the flexoelectric invariant [12]

$$\beta' E_z n_z \left( \frac{\partial n_x}{\partial x} + \frac{\partial n_y}{\partial y} \right), \tag{1}$$

where the director components are $n_x = \theta \sin\varphi \approx \theta\varphi$, $n_y = \theta \cos\varphi \approx \theta$, $n_z \approx 1 - \theta^2$, it is assumed that the tilt angle $\theta$ and the azimuth angle $\varphi$ are small, and $\beta'$ is the flexoelectric coefficient. We assume the electric nature of the field $E$. For example, such a field can be created by the elastic stress $\sigma$ at the expense of increasing the density of the surface charge at decreasing surface area of polar heads of molecules. For free-standing thin films, the elastic stress can be provoked by the film weight $w$ if the film thickness, i.e., the number of smectic layers $N$ ($w \sim N$), is sufficiently large and thus $E \sim \sigma \sim w \sim N$.

The general expression for the free-energy density in thin smectic-$C$ film under consideration can be written in the form

$$F = t n_z^2 \left(n_x^2 + n_y^2\right) + \frac{1}{4} a n_z^4 \left(n_x^2 + n_y^2\right)^2 + \frac{1}{2} K' n_z^2 \left( \frac{\partial n_x}{\partial x} + \frac{\partial n_y}{\partial y} \right)^2 + \frac{1}{2} K'' n_z^2 \left( \frac{\partial n_x}{\partial y} - \frac{\partial n_y}{\partial x} \right)^2$$

$$+ \frac{1}{\chi} P_z^2 + \frac{1}{2} G \left[ \left( \frac{\partial P_z}{\partial x} \right)^2 + \left( \frac{\partial P_z}{\partial y} \right)^2 \right] + \left( \frac{2\beta'}{\chi} \right) P_z n_z \left( \frac{\partial n_x}{\partial x} + \frac{\partial n_y}{\partial y} \right) - P_z E_z + \sigma_{xx} n_x^2 , \tag{2}$$

where the first two terms describe the Sm-$A$–Sm-$C$ phase transition in a homogeneous smectic film; they can be written also in the form $t\theta^2 + (a/4)\,\theta^4$, which results in the homogeneous tilt angle $\theta_0 = \sqrt{-2t/a}$. The next two terms describe the elastic energy of orientational deformations in the smectic plane $xy$, the constants $K'$ and $K''$ being the corresponding elastic moduli; the terms in Eq. (2) containing the polarization component $P_z$ describe the possibility of the existence of the polarization due to the presence of in-plane director modulations (flexoelectric effect) and due to the action of the external electric field perpendicular to the smectic plane, the constant $\chi$ being positive because of the absence of a homogeneous spontaneous polarization, the positive constant $G$ and the corresponding term describe the inhomogeneous part of free-energy related to the polarization presence. The last term in Eq. (2) describes the effect of anisotropic part of the elastic energy, the stretch being directed along the $x$ axis of the free-standing film, for example, perpendicularly to the frames supporting the smectic-$C$ film. If one neglects the effects of polarization inhomogeneity (for example, at small values of $G$) but takes into account the flexoelectric effect, then the minimization of $F$ with respect to $P_z$ results in the term described by Eq. (1).

Let us consider a free-standing smectic film at the conditions when its weight causes the mechanical stress component $\sigma_{xx}$ and the perturbations $\theta' = \theta - \theta_0$ and $\varphi$, which are homogeneous along the $y$ axis but heterogeneous along the $x$ axis (when the supporting frames are directed along the $y$ axis); the values $\theta = \theta_0$ and $\varphi = 0$ correspond to a nonperturbed smectic-$C$ phase. In such a case, one should take into account the following approximations in the free-energy density [see Eq. (2)]:

$$\sigma_{xx} n_x^2 \approx g w \theta_0^2 \varphi^2, a\theta_0^2 \theta'^2, \frac{1}{2} K \theta_0^2 \left(\frac{\partial \varphi}{\partial x}\right)^2, \frac{1}{2} b \left(\frac{\partial \theta'}{\partial x}\right)^2,$$

where the constants $g, a$, $K = K' - \beta'^2 \chi^{-1}$, and $b = K''$ are positive. The positiveness of $K$ takes place at sufficiently small values of the flexoelectric coefficient $\beta'$. At large values of $\beta'$, one should consider the possibility of spontaneous in-plane flexoelectric modulations. For a simplicity, we neglect effects of free charges, internal fields, and boundaries. The invariant (1) can be written in the form

$$\beta w \theta_0^2 \theta' \frac{\partial \varphi}{\partial x}, \tag{3}$$

which results in a nonzero free-energy value after the integration over $x$ coordinate, here $\beta' E \sim \beta w$, the coefficient $\beta$ being proportional to the permanent dipole moment and concentration of polar molecules.

The sum of terms discussed above determines the free-energy density in the framework of the considered approximation and results, after its minimization with respect to $\theta'$ and $\varphi$, in the following equations for the distributions $\theta'(x)$ and $\varphi(x)$:

$$2a\theta_0^2 \theta' - b \frac{\partial^2 \theta'}{\partial x^2} + \beta w \theta_0^2 \frac{\partial \varphi}{\partial x} = 0, \tag{4}$$

$$2gw\varphi - K \frac{\partial^2 \varphi}{\partial x^2} - \beta w \frac{\partial \theta'}{\partial x} = 0. \tag{5}$$

The solutions of Eqs. (4) and (5) can be written in the form $\theta'(x) = A \sin(qx)$ and $\varphi = B \cos(qx)$, where nonzero values of the amplitudes $A$ and $B$ exist if the characteristic equation

$$\left(2a\theta_0^2 + bq^2\right)\left(2gw + Kq^2\right) = \beta^2 \theta_0^2 q^2 w^2 \tag{6}$$

has the physical solution $w\left(q^2\right)$ for positive values of $q^2$,

$$w\left(q^2\right) = \frac{g\left(2a\theta_0^2 + bq^2\right) + \sqrt{g^2\left(2a\theta_0^2 + bq^2\right)^2 + K\beta^2\theta_0^2 q^4\left(2a\theta_0^2 + bq^2\right)}}{\beta^2 \theta_0^2 q^2}. \tag{7}$$

The function $w\left(q^2\right)$ has the minimum value $w_{cr} = w\left(q_{cr}^2\right)$,

$$w_{cr} = \frac{gb}{2\beta^2\theta_0^2}\left[1 + \sqrt{1 + 2\left(2aK\right)^{1/2}\left(|\,\beta\,|\,\theta_0^2/bg\right)}\right]^2 \tag{8}$$

at the value of wave number squared $q^2 = q_{cr}^2$,

$$q_{cr}^2 = \frac{1 + \sqrt{1 + 2\left(2aK\right)^{1/2}\left(|\,\beta\,|\,\theta_0^2/bg\right)}}{\left(K/2a\right)^{1/2}\left(|\,\beta\,|\,/g\right)}. \tag{9}$$

The magnitude $w$ is positive for positive values of $g$. For negative $g$, the magnitude $w$ has the opposite sign, but the same absolute value. In the last case, one should change the sign on the right-hand sides of Eqs. (7) and (8) and write the absolute value of $g$ in equations (7)–(9). Expressions (6)–(9) show that there is the threshold weight value $w = w_{cr}$ (or critical number of layers $N_{cr}$) for the smectic-$C$ film, above which the one-dimensional in-plane modulation (stripe state) can appear with the threshold wave number $q_{cr}$ (the spatial period $h_{cr}$ being equal to $2\pi q_{cr}^{-1}$). The threshold $w_{cr}$ substantially depends on the flexoelectric coefficient $\beta$ and the tilt angle $\theta_0$,

$$w_{cr} \sim N_{cr} \sim \frac{1}{\beta^2\theta_0^2} \sim \frac{1}{\beta^2\left(T_{AC} - T\right)}, \tag{10}$$

i.e., the values $w_{cr}$ and $N_{cr}$ must strongly increase near the phase transition temperature $T_{AC}$, where $\theta_0^2 \sim (T_{AC} - T)$. At a fixed weight $w$, Eq. (7) determines the corresponding critical temperature $T_{cr}$ below which the stripe state arises,

$$\left(T_{AC} - T_{cr}\right) \sim \frac{1}{\beta^2 w} \sim \frac{1}{\beta^2 N}. \tag{11}$$

## V. DISCUSSION

The theory presented gives a qualitatively good explanation for the properties of the stripe phase. Expressions (8)–(11) describe the observed $N/T$ phase diagram (Fig. 2), the $N_{\rm cr}$ dependence on the spontaneous polarization $P_s$ at a fixed temperature (Fig. 8) ($P_s$ must be proportional to the permanent dipole moment and the concentration of polar molecules, i.e., $P_s \sim \beta$), and the concentration dependence of $(T_{AC} - T_{\rm cr})$ (Fig. 11). In general, the magnitude of $\beta$ as a function of $P_s$ and $E_z$ as a function of $N$ is determined up to corresponding constants. This is the reason why for the comparison with experimental data one should rewrite Eqs. (10) and (11), in the form of Eqs. (12) and (13). Figure 12 shows a fit of the dependence of $(T_{AC} - T_s)$ on the number of layers for different chiral-racemic mixtures of $C7$:

$$T_{AC} - T_s = T_0 + \frac{1}{\beta^2 (N - N_0)}, \tag{12}$$

where $T_0, \beta, N_0$ are constants. The fitting parameters for 100% chiral $C7$ are the following: $T_0 \approx 0.2K, \beta^2 = 1.4 \times 10^{-3} K^{-1}$, and $N_0 = 15$. The difference between $N_0$ and $N_{\rm cr}$ exists because the Sm-$C^*$–Sm-$G$ phase transition takes place before the $N_0$ is achieved.

The solid curve on Fig. 8 shows the fitting results of the experimental dependence $N_{\rm cr}(P)$ with an expression

$$N_{\rm cr} = \frac{\alpha}{(P - P_s^0)^2}, \tag{13}$$

where $\alpha$ and $P_s^0$ are constants. We have obtained $\alpha = 6.9 \times 10^5$ (nC/cm$^2$)$^2$, $P_s^0 = 65.8$ nC/cm$^2$. In both cases the theoretical curves give a good description of the experimental results.

One can see that small concentrations of the chiral component, i.e., small coefficients $\beta$, provoke steep functions $T_{\rm cr}(N)$. It is curious that the concentration dependence of the spontaneous polarization at the stripe formation temperature $T_{\rm cr}$ must be absent in the considered approximation, i.e., $P_s(\beta)_{T=T_{\rm cr}} \sim \beta\theta_0(T_{\rm cr}) \sim \beta (T_{AC} - T_{\rm cr})^{1/2} \sim$const, in accordance with the experimental data (Fig. 9). Equation (8) shows that the temperature dependence of the interstripe distance $h_{\rm cr} \sim q_{\rm cr}^{-1}$ is an increasing function of temperature, but $h_{\rm cr}$ has no critical divergence at $T = T_{AC}$, in accordance with the experimental data (Fig. 6). The last conclusion is related to the dependence of the first term in Eq. (2) on the magnitude $w$. If such a dependence is absent, for example, at some constant anisotropy of the surface pressure, one can conclude from the corresponding equations (4) and (5) that the wave number squared would be proportional to the tilt angle, i.e., the distance between stripes would have a critical divergence at the phase transition temperature.

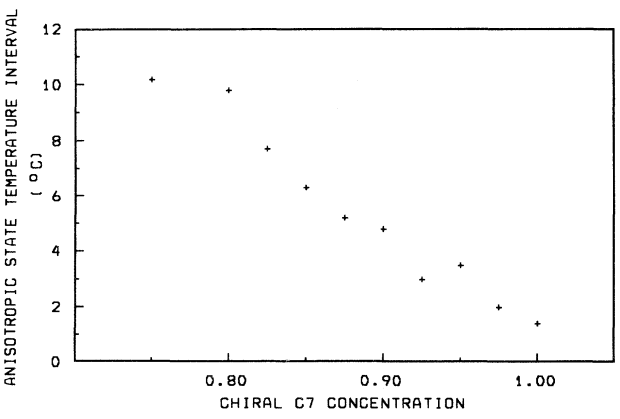


FIG. 11. Concentration dependence of the anisotropic state temperature interval taken at $N$=700.

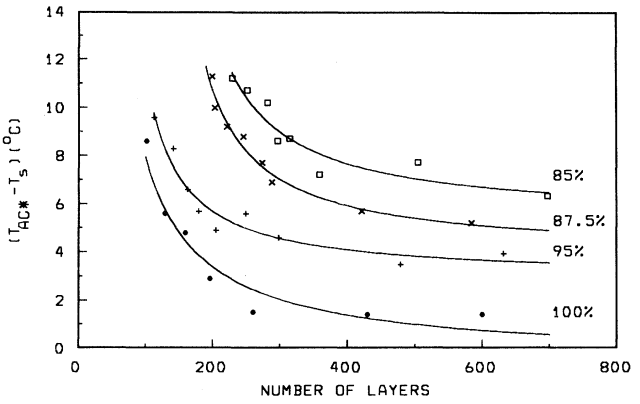


FIG. 12. Fitting of the dependence of the stripe state formation temperature $T_s$ on the number of layers with the expression (12).

Thus the proposed phenomenological approach can explain some characteristic features of the stripe state formation in thin smectic-$C$ films with sufficiently strong polar properties (with large flexoelectric coefficient). In fact, the flexoelectric instability of such films with a fixed phase transition temperature $T_{AC}$ was described above. In general, the $T_{AC}$ point can be a function of the number of smectic layers $N$ and can be influenced by free charges and internal fields, i.e., the real situation can be more complex [12]. Besides, the spontaneous two-dimensional in-plane modulation of smectic-$C$ films can take place if the flexoelectric coefficient $\beta'$ is larger than the critical value $\beta'_{\rm cr} \approx \sqrt{\chi K'}$, as mentioned above.

According to our model, the stripe state disappears in thin layers because the electric field $E_z$ is not strong enough to produce stripes. This explains the similarity of images of the anisotropic state in thick films before the stripes are formed and that of sealed ultrathin films with thicknesses below $N_{\rm cr}$. In films, where $E_z$ is small, periodic structures can also be formed in accordance with mechanisms proposed in [25]. In this case a spontaneous formation of quadratic lattice was predicted, where the polarization charge in the center of the quadrats is zero. This prediction corresponds to the metastable chessboard texture observed in [14].

The textures observed in achiral and chiral smectic films show many similarities. The chessboard texture

is topologically equivalent to the brick wall and honeycomb textures observed in [15, 16]. Figure 3 shows a metastable aperiodical stripe texture of ultrathin chiral $C7$ films, which is analogous to stripes in achiral films [15, 16] because the contrast inside of stripes is constant.

The experimentally observed difference between chiral and achiral films is that the stable configuration of ultrathin chiral ferroelectric films is the spontaneously anisotropic texture with an excellent quality of uniaxial orientation. The loss of correlation in orientation in films with decreasing spontaneous polarization is continuous and in the 50% chiral $C7$ mixture we observed a classic schlieren texture for the anisotropic state. The dipolar interaction is probably responsible for unusual properties of free-standing ultrathin films, especially for the occurrence of the anisotropic state [11].

The stripe state patterns observed in the antiferroelectric phase are similar to the smectic-$C^*$ phase, which can also be regarded in the framework of the present model. The increase of the stripe periodicity in the Sm-$C_A$ phase with respect to the Sm-$C^*$ phase can be explained by lower electric field $E_z$ due to the antiferroelectric structure, because from our experimental observations it follows that the antiferroelectric phase behavior is analogous to the $C7$ mixtures with lower spontaneous polarization. The results of this paper show that mechanisms of the stripe formation in chiral and achiral films are different. The $C7$ stripe is a bulky periodical texture which stability is definitively related to the value of spontaneous polarization.

## ACKNOWLEDGMENTS

The authors are grateful to Dr. A. Yoshizawa for supplying us with the substance $Y1$, to the Deutsche Forschungsgemeinschaft, to the Fonds der Chemischen Industrie (Germany), and to Russian Foundation of Fundamental Research (S.A.P.) for financial support.

[1] C. Rosenblatt, R. Pindak, N.A. Clark, and R.B. Meyer, Phys. Rev. Lett. **42**, 1220 (1979).
[2] C. Rosenblatt, R.B. Meyer, R. Pindak, and N.A. Clark, Phys. Rev. A **21**, 140 (1980).
[3] R. Pindak, C. Young, R.B. Meyer, and N.A. Clark, Phys. Rev. Lett. **45**, 1193 (1980).
[4] J.D. Brock, R.J. Birgenau, J.D. Litster, and A. Aharony, Contemp. Phys. **30**, 321 (1989).
[5] P. Pieranski *et al.*, Physica A **194**, 364 (1993).
[6] C.C. Huang and T. Stoebe, Adv. Phys. **42**, 343 (1993).
[7] S. Heinekamp, R. Pelkovits, E. Fontes, E. Yi Chen, R. Pindak, and R. Meyer, Phys. Rev. Lett. **52**, 1017 (1984).
[8] Ch. Bahr and D. Fliegner, Phys. Rev. A **46**, 7657 (1992).
[9] I. Kraus, P. Pieranski, E. Demikhov, and H. Stegemeyer, Phys. Rev. E **48**, 1916 (1993).
[10] D.R. Nelson and R.A. Pelcovits, Phys. Rev. B **16**, 2191 (1977).
[11] R.A. Pelcovits and B.I. Halperin, Phys. Rev. B **19**, 4614 (1979).
[12] S.A. Pikin, *Structural Transformations in Liquid Crystals* (Gordon and Breach, New York, 1991), p. 229.
[13] Ch. Bahr and D. Fliegner, Phys. Rev. Lett. **70**, 1842 (1993).
[14] E. Demikhov, Europhys. Lett. **25**, 259 (1994); E. Demikhov and H. Stegemeyer, Liq. Cryst. **18**, 37 (1995).
[15] J.E. Maclennan and M. Seul, Phys. Rev. Lett. **69**, 2082 (1992).
[16] J.E. Maclennan, U. Sohling, N.A. Clark, and M. Seul, Phys. Rev. E **49**, 3207 (1994).
[17] J.V. Selinger, Z.-G. Wang, R.F. Bruinsma, and C.M. Knobler, Phys. Rev. Lett. **70**, 1139 (1993).
[18] E.I. Demikhov, Phys. Rev. E **51**, 1 (1995).
[19] J. Ruiz-Garsia, X. Qiu, M.-W. Tsao, G. Marshall, C.M. Knobler, G. Overbeck, and D. Möbius, J. Phys. Chem. **97**, 6955 (1993).
[20] G.A. Overbeck, D. Hönig, and D. Möbius, Thin Solid Films **242**, 213 (1994).
[21] S. Riviere, S. Henon, and J. Meuner, Phys. Rev. E **49**, 1375 (1994).
[22] E. I. Demikhov and S. A. Pikin, JETP Lett. **61**, 666 (1995).
[23] S.A. Langer and J.P. Sethna, Phys. Rev. A **34**, 5035 (1986).
[24] G.A. Hinshaw, R.G. Petschek, and R.A. Pelcovits, Phys. Rev. Lett. **60**, 1864 (1988).
[25] S.A. Pikin, A. Sparavigna, and A. Strigazzi (unpublished).
[26] Ch. Bahr and G. Heppke, Mol. Cryst. Liq. Cryst. **148**, 29 (1987); B.R. Ratna, R. Shashidhar, Geetha G. Nair, S. Krishna Prasad, Ch. Bahr, and G. Heppke, Phys. Rev. A **37**, 1824 (1984).
[27] M. Born and E. Wolf, *Principles of Optics* (Pergamon, Oxford, 1980), Chap. 7.6, p. 327.
[28] A. Yoshizawa, I. Nishiyama, M. Fukumasa, T. Hirai, and M. Yamane, Jpn. J. Appl. Phys. **28**, L1269 (1989).

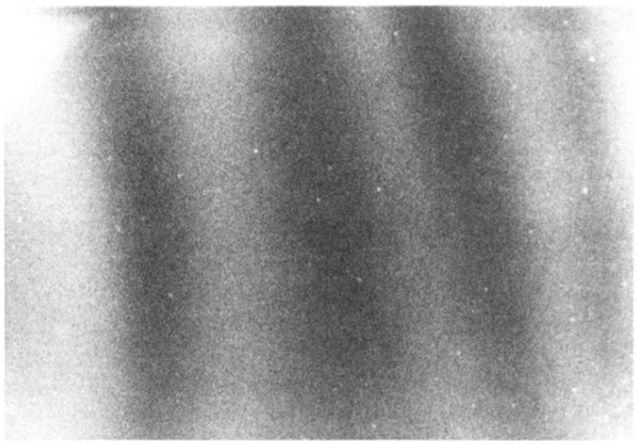

FIG. 10. Stripe state in an antiferroelectric phase of $Y1$.

FIG. 3. Metastable anisotropic texture in a 25-layer film at $T = 48.06\,^{\circ}\mathrm{C}$.

(a)

(b)

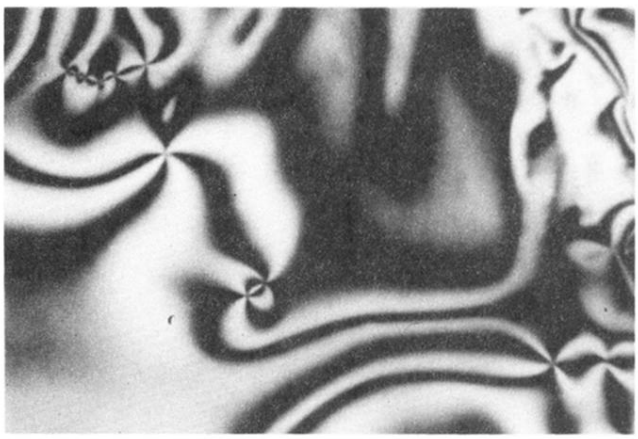

(c)

FIG. 4. (a) Anisotropic texture of a $N=30$ smectic-$C^*$ film of 100% chiral $C7$ at $T = 48.06\,^{\circ}\mathrm{C}$. (b) Anisotropic smectic-$C^*$ texture of an $N=150$ film of 87.5% chiral $C7$ mixture at $T = 53.85\,^{\circ}\mathrm{C}$; (c) Schlieren texture of thick films ($\sim$ 500 layers) in a mixture with 50% chiral $C7$ at $T = 50.05^{\circ}\mathrm{C}$.

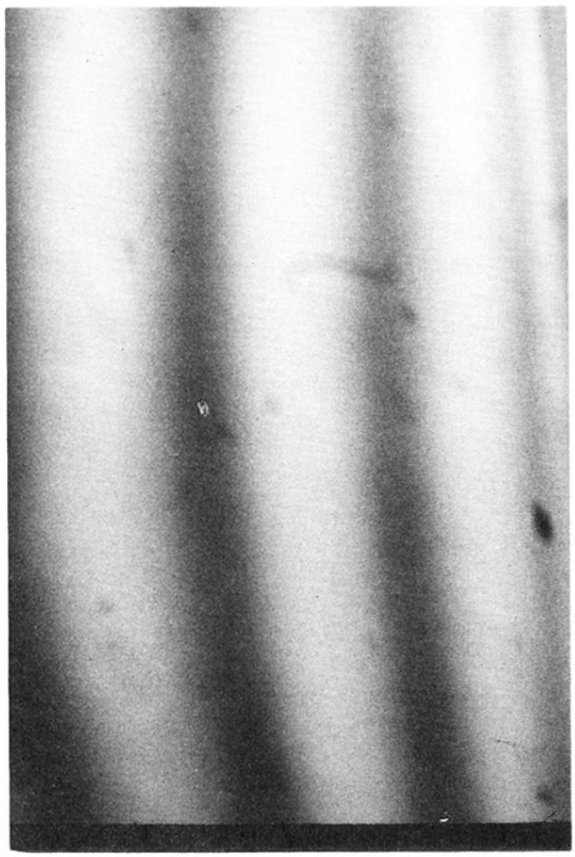

FIG. 5. Striped state of the plane director field of the smectic-$C^*$ phase in an $N=400$ film of chiral $C7$.